Erschienen in: Progress in Photovoltaics : Research and Applications ; 12 (2004), 5. - S. 355-363
https://dx.doi.org/10.1002/pip.555

Light-modulated Lock-in Thermography for Photosensitive pn-Structures and Solar Cells

M. Kaes*,†, S. Seren, T. Pernau and G. Hahn
University of Konstanz, Department of Physics, P.O. Box X916, 78457 Konstanz, Germany

Lock-in thermography (LIT) is a well-established tool for defect analysis of solar cells, but so far has been restricted to the measurement of metallized samples. The new light-modulated lock-in thermography (LimoLIT) described in this paper overcomes this restriction by generating the voltage modulation needed for detection from photovoltaic conversion of modulated light. Thus wafers can be measured during all stages of fabrication, a pn-junction provided. The contactless LimoLIT method shows a stronger measurement signal and invokes a current flow close to illuminated operating conditions of solar cells, whereas conventional LIT is only comparable to a dark I–V measurement. Copyright © 2004 John Wiley & Sons, Ltd.

KEY WORDS: thermography; lock-in; shunt; contactless; multicrystalline; silicon; infrared

INTRODUCTION

Thermographic investigations of solar cells in general can be used to detect weak current leaks at defects and impurities or process-induced damage due to their local heat generation. Areas of the specimen containing such defects, as appearing frequently in multicristalline (mc) silicon for example, may deteriorate the device quality. The detection can be performed by measuring the lateral temperature distribution of a sample with an infrared (IR) sensitive camera.[1,2] To raise the signal-to-noise ratio for detection of temperature variations in the 10 μK range usually a lock-in technique based on an externally modulated voltage via the metal contacts of the solar cell is applied. This is the well-known lock-in thermography (LIT), later named voltage-modulated lock-in thermography[3,4] (VomoLIT) which also enhances the lateral resolution of the shunts. However, with VomoLIT a metallization of the solar cell is coercibly required. As this is one of the last steps in the fabrication process of solar cells, thermographic analysis of shunts so far has been restricted to measurements at the end of the solar cell process.

Light-modulated lock-in thermography (LimoLIT) is a new measurement technique which allows the detection of heat-dissipating areas as a result of microscopic short-circuits (shunts) in *pn*-structures as well as in solar cells. By means of LimoLIT, semiconductor devices and solar cells in particular can be characterized in every stage of the manufacturing process, regardless of the existence of any electric contacts, given only the presence of a *pn*-junction. This enables process monitoring, even in the early stages of processing. Further on this allows

* Correspondence to: M. Kaes, University of Konstanz, Department of Physics, P.O. Box X916, Konstanz, Germany.
†E-mail: martin.kaes@uni-konstanz.de

Contract/grant sponsor: EC; contract/grant number: ENK6-CT-2001-00574.
Contract/grant sponsor: BMU; contract/grant number: 0329846J.

one to track the development of shunts during individual fabrication steps of solar cells. The danger of a possible contamination of the sample is negligibly small as the method is contactless.

LimoLIT uses intensity-modulated light generating excess charge carriers as a substitute for the externally applied lock-in signal. With this new technique heat-dissipating defects in solar cells can be localized at operating point conditions by the choice of an appropriate bias light, revealing the defects occurring during normal operation.

In this paper we focus on some features of this new technique. A comparison with the standard VomoLIT method and first results of a shunt monitoring experiment will be presented.

EXPERIMENTAL SET-UP

In the conventional VomoLIT the reference signal is generated by an AD/DA interface card (part of the computer) and amplified by an external power amplifier. This signal is applied to the solar cell by a probe via the front finger grid and the back-surface metallization. The solar cell is fixed by vacuum on a temperature-stabilized metal table. The IR-sensitive camera mounted directly above (camera type JADE II MWIR by Cedip, distributed by InfraTec, sensitive in the 3–5 μm range) provides temperature images (320×256 pixel) of the solar cell at discrete adjustable time intervals (typically 8 ms). The sensor of the camera is kept at 78 K by a Stirling cooler, which gives a noise level of $\sigma_k \simeq 20$ mK without any lock-in technique. The frames are collected by a frame grabber card (inside the computer). The subsequent two-channel lock-in calculation is performed by the computer, as well as various control functions. The computer is controlled by a self-developed software. Feeding a temperature signal:

$$T(t) = A\exp(\mathrm{i}(\omega t - \phi)), \quad \phi = \phi_{\text{system}} + \phi_{\text{signal}} \tag{1}$$

by the two-channel lock-in process results in:

$$A_{90^\circ} = A\sin(\phi_{\text{signal}}) \qquad \text{and} \qquad A_{0^\circ} = A\cos(\phi_{\text{signal}}) \tag{2}$$

The system phase delay ϕ_{system} can be determined and corrected by measuring a periodic homogeneously heated surface with an expected signal phase delay ϕ_{signal} of $\pi/2$.

The thermographic images presented in this paper show the magnitude which is phase independent:

$$A(x,y) = \sqrt{A^2_{90^\circ}(x,y) + A^2_{0^\circ}(x,y)} \tag{3}$$

When processing N images with the lock-in technique, the noise level σ is reduced to

$$\sigma = \sigma_k\sqrt{\frac{2}{N}} \tag{4}$$

Owing to the exponential decay of thermal waves, the phase-sensitive lock-in technique achieves a better lateral resolution compared with a steady-state technique.[4] The phase delay detected by the lock-in calculation corresponds to a time delay of the signal which represents additional information.[5,6]

Because of the nonuniform emissivity of silicon in the 3–5 μm range the real surface temperature variations of the solar cell are expected to be slightly higher than the measured $A(x, y)$-values. If desired this effect can either be measured and corrected in the image calculation or eliminated by covering the measured cell surface with a thin foil with uniform emissivity.[3] Only a small difference could be detected by using such a foil, except for signals at the metallization, therefore the measurements have been carried out without the foil neglecting the influence of the nonuniform emissivity. However, the temperature calibration of the camera is done with the help of a black painted surface with high emissivity. For calibration its temperature is measured by the camera as well as by a contacted Peltier element at different temperatures under steady-state conditions.

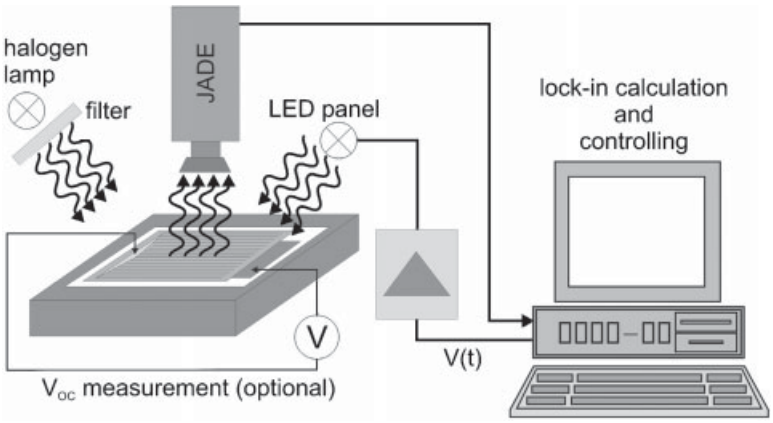

Figure 1. Experimental set-up of the LimoLIT measurement assembly. The wafer with a *pn* junction or the solar cell can be illuminated by a halogen lamp (constant-bias light). The modulated reference signal (pulsed light) is provided by an array of LEDs. Different wavelengths can be used

For LimoLIT measurements (Figure 1), the power amplifier is connected to a light source suitable for modulation (kHz range). In our set-up this is realized by a LED array. The array illuminates the wafer containing a *pn*-junction or the solar cell from the front or the back surface. The adjustable bias light source is realized by a halogen lamp. An IR absorbing filter is attached to minimize direct IR (3–5 μm) irradiation of the solar cell. Optionally, electrical contacting can be used to measure the light-generated voltage on metallized solar cells and to adjust the applied voltage via the incident light intensity.

VomoLIT–LimoLIT COMPARISON

Unbiased measurement

In the following, we seek to demonstrate the possibilities of the LimoLIT method. For a comparison between the conventional VomoLIT and the LimoLIT, Figure 2 shows two measurements using a modulation frequency of 12·5 Hz on the same sample.

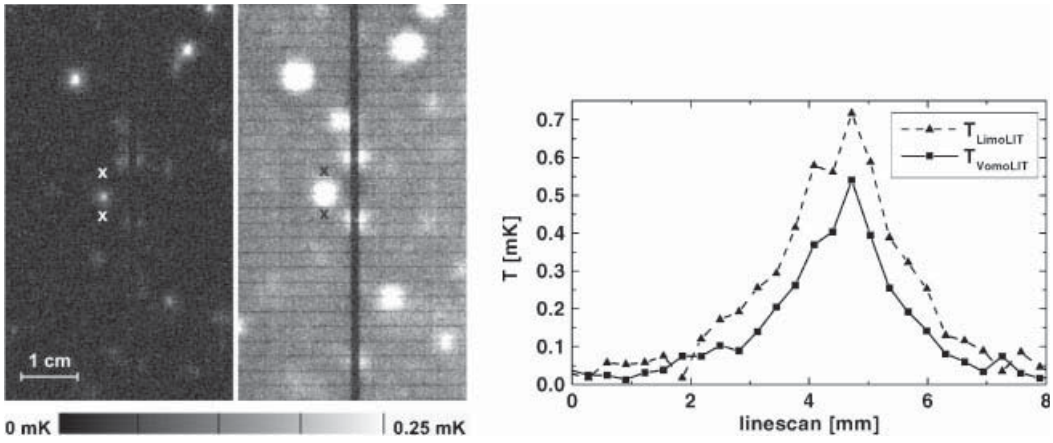

Figure 2. Conventional VomoLIT measurement of a multicrystalline silicon solar cell in forward direction without additional bias voltage (left image, left) and LimoLIT measurement (wavelength for illumination: 880 nm) of the same cell also without a bias light (same scaling, left image, right). Measurement time for both measurements was 10 h. The linescans across the marked region shown in the right illustration demonstrate the higher sensitivity of the LimoLIT measurement. For comparison of the linescans the background signal is subtracted from the LimoLIT signal

On the left-hand side of Figure 2 a section of a mc-silicon solar cell with screen-printed contacts and conventional VomoLIT can be seen. The picture on the right shows the same area with the LimoLIT method. The amplitude (320 mV) and shape (square wave) of the modulated bias was identical for both measurements. In both measurements heat-dissipating shunts are clearly visible, which reduce the performance of this solar cell. Both mappings are scaled identically to demonstrate the equivalence of the measurement methods. The thermalization results in a constant-background signal for the LimoLIT measurement. The LimoLIT signal of the shunts is stronger than the conventional VomoLIT signal.

The VomoLIT method uses an external voltage to inject a current into the sample under investigation. Injected carriers are mainly majority carriers, as only few of them will flow across the space-charge region. This avoids a background signal from recombination of minority carriers, but the resulting operating behaviour of the solar cell is only comparable to a dark *I–V* measurement. The LimoLIT method however represents the real operation conditions of a solar cell, as all electronic processes are running in the sample, bulk recombination included. Especially the current distribution is different from VomoLIT.

Neglecting the contact resistance, the metal potentials of the metallized solar cell (front and back surfaces) are equal to the corresponding Fermi levels $E_{\mathrm{F},n}$ and $E_{\mathrm{F},p}$ in the semiconductor (emitter and base) which have the potential difference U. Under forward bias there are three Peltier effects possible:

$$\text{metal–emitter (Peltier cooling)}: \; P_{\mathrm{ME}} = -\frac{I_{\mathrm{sh}}}{e}\left(E_{\mathrm{C},n} - E_{\mathrm{F},n}\right) \tag{5}$$

$$\text{emitter–base (Peltier heating)}: \; P_{\mathrm{BE}} = \frac{I_{\mathrm{sh}}}{e}\left(E_{\mathrm{C},n} - E_{\mathrm{F},n} + E_{\mathrm{F},p} - E_{\mathrm{V},p}\right) = \frac{I_{\mathrm{sh}}}{e}\left(E_{\mathrm{g}} - eU_{\mathrm{D}}\right) \tag{6}$$

$$\text{base–metal (Peltier cooling)}: \; P_{\mathrm{BM}} = -\frac{I_{\mathrm{sh}}}{e}\left(E_{\mathrm{F},p} - E_{\mathrm{V},p}\right) \tag{7}$$

(P power; I_{sh} shunt current; e elementary charge; $E_{\mathrm{C},n/p}$ conduction band energy level in n/p-region; $E_{\mathrm{V},n/p}$ valence band energy level in n/p-region; $E_{\mathrm{F},n/p}$ Fermi energy level in n/p-region; U_{D} diffusion voltage; E_{g}: band-gap energy).

These Peltier effects can either be laterally separated, e.g., for local back contacts, or stacked vertically in case of a shunt located underneath a grid finger and full area back-surface metallization. For vertical stacking of the Peltier heat source and sinks the net heat generation is simply the joule heating $P = I_{\mathrm{sh}}U$. In contrast to VomoLIT where the current is injected and mainly transported to the shunt via the metallization, in LimoLIT the current can be effectively transported by the semiconductor itself. Thus in LimoLIT the Peltier heating and cooling is expected to be widespread compared with VomoLIT, depending on the lumped series resistance and the resulting current distribution.

Therefore the Peltier effect can lead to a difference in LimoLIT and VomoLIT of maximum

$$P_{\mathrm{LimoLIT}} - P_{\mathrm{VomoLIT}} = \frac{I_{\mathrm{sh}}}{e}\left(E_{\mathrm{g}} - eU_{\mathrm{D}}\right) \tag{8}$$

Assuming $E_{\mathrm{g}} = 1{\cdot}1$ eV, $U_{\mathrm{D}} = 720$ mV, and $U = 320$ mV, the maximum LimoLIT signal is double the VomoLIT signal. For the shunts marked in Figure 2 the signal strength in the LimoLIT measurement is increased by about 50%.

Depending on shunt strength and carrier transportation, a local shunt will drain the carriers from its surroundings. For stronger shunts in unmetallized cells this can be seen as a decreased background signal in the cell area affected by the shunt (see left-hand wafer in Figure 5, lower right-hand corner). Owing to decreasing series resistance after metallization, individual shunt signals are supposed to be increased because of improved carrier transportation to the shunts.

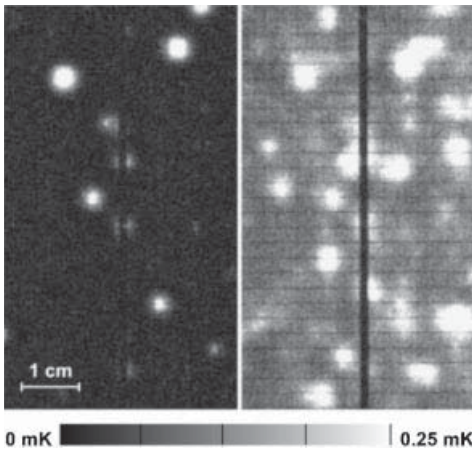

Figure 3. Conventional VomoLIT measurement of the solar cell shown in Figure 2 in forward direction with a constant-bias voltage applied (left). LimoLIT measurement of the same cell with a constant-bias light, realized with an adjustable light source (right). Measurement time was 10 h as in Figure 2

Biased measurements

Measurements performed without the presence of an additional constant-bias signal cannot demonstrate the leakage power behaviour of solar cells under realistic operating conditions. There is a need to induce a charge carrier concentration close to maximum power point operation under sunlight.

The DC bias is realized by applying: (a) a constant forward voltage in the case of the conventional VomoLIT; or (b) a constant white light source together with the LimoLIT technique. The bias light power can be regulated for best adjustment to the working point of the device under investigation. Figure 3 shows the same sample as presented in Figure 2 with an additional constant bias ($U_{\mathrm{bias}} = 400\,\mathrm{mV}$). The modulation (50 mV, 12·5 Hz) is the same as for the measurement shown in Figure 2.

The DC-biased measurement is not a large signal or integral measurement any more, but a small signal or differential technique. Whereas integral thermography detects $P = U^2/R$, the differential method measures $\mathrm{d}P = (\mathrm{d}U)^2/\mathrm{d}R$ which is obviously more sensitive to nonlinearities occurring right at the operation level U_{bias}. This is the reason why the biased measurements in Figure 3, and especially the light-biased LimoLIT measurement, reveal details which are not visible in the unbiased measurements of Figure 2. This can be explained with the different nature of the visualized shunt types. Whereas linear ohmic shunts are visible even without a constant bias, nonlinear Schottky-type shunts appear stronger under a constant forward bias because of the exponentially decreasing differential resistance. This allows better selectivity for the investigation of different shunt types.

Although biased lock-in thermography is a differential measurement, the situation of a constant bias is the more realistic scenario for a solar cell, as it is closer to steady-state operating conditions. However, to achieve most meaningful results it is necessary to perform multiple measurements at various bias levels and to calculate the true integral behaviour as discussed elsewhere for quantum efficiencies[7,8] and for lifetime measurements.[9]

Net result

For LimoLIT the light-induced current direction across the space-charge region is opposite to the current flow observed in conventional VomoLIT. The current direction in LimoLIT is the same as for illuminated operation of the solar cell. For LimoLIT the Peltier effect increases sensitivity. The LimoLIT technique is closer to standard operation conditions compared with VomoLIT, and provides a realistic assessment of the impact of shunts on solar cell performance.

For *pn*-structures the LimoLIT method can be applied to measure samples at bias in the forward direction not exceeding the diffusion voltage. The set-up also allows measurements in a look-through geometry.

WAVELENGTH-DEPENDENT GENERATION AND THERMALIZATION

Where the conventional VomoLIT is constricted to the signal envelope, frequency, and amplitude invoked by the periodical bias signal, the LimoLIT method offers in addition a variation of the light wavelength by using light sources of different colours. This allows a selective signal generation depending on the spectral response and absorption of the investigated material.

In contrast to conventional VomoLIT, the LimoLIT produces a signal background from the illumination. Excess quantum energy of the absorbed photons is converted either into free carrier emission or phonons (thermalization). The thermal relaxation is rather fast (10^{-11} s) and the resulting heat is proportional to the excess photon energy. It is therefore advisable to use wavelengths as long as possible for illumination because, e.g., at a photon wavelength of 551 nm the photon excess energy equals the energy absorbed by the silicon. Inhomogeneous carrier generation from locally varying absorption properties contributes directly to the thermalization background signal. But for typical shunts which are supposed to reduce cell efficiency this does not significantly affect the shunt-to-background ratio.

Another source for a homogeneous signal offset can be the recombination of generated electron–hole pairs under emission of photons (photoluminescence). This is relevant only for direct semiconductors. In the case of indirect semiconductors (like silicon) the phonon-assisted recombination at impurities is an additional inhomogeneous heat source.

Moreover, the carriers accelerated by crossing the space-charge region convert their kinetic energy into phonons. The homogeneous offset signal generally shows a constant phase delay of 90° and can therefore be eliminated quite easily with a phase-sensitive filter or by displaying the 0° signal, if desired.

For further investigations, linescans between the marked points in Figure 2 were performed for three different wavelengths for excitation, resulting in comparable carrier concentrations. Results can be seen in Figure 4.

Obviously, the signal-to-background ratio is best for the IR light source (880 nm), as the least excess photon energy produces the lowest heat by thermalization. With increasing photon energy, the signal-to-noise ratio decreases, as can be seen for the shorter wavelengths (609 and 505 nm, compare peak signal and background). The dips of the signal visible in Figure 4 are due to the metal grid fingers. The direct light reflection of the metal is not detected, as the infrared camera is not sensitive in this wavelength regime.

SHUNT MONITORING

Two solar cells were processed, one from a Czochralski (Cz) and the other from a mc-silicon wafer, both using a standard firing through SiN_x process with screen-printed contacts.[10] After double-sided $POCl_3$ emitter diffusion the wafers were intentionally damaged by scratching and afterwards measured by the LimoLIT method with

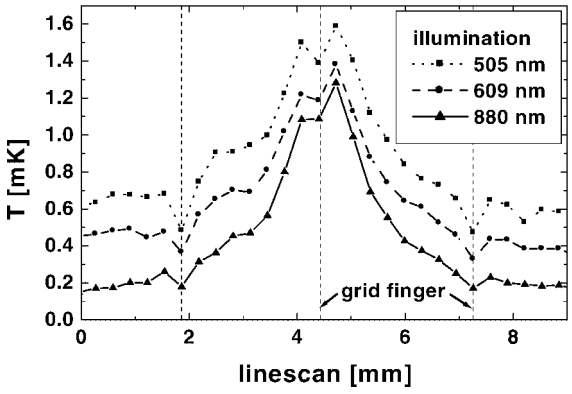

Figure 4. Linescans across the shunt region marked in Figure 2 using the LimoLIT technique with different wavelengths as lock-in signal sources

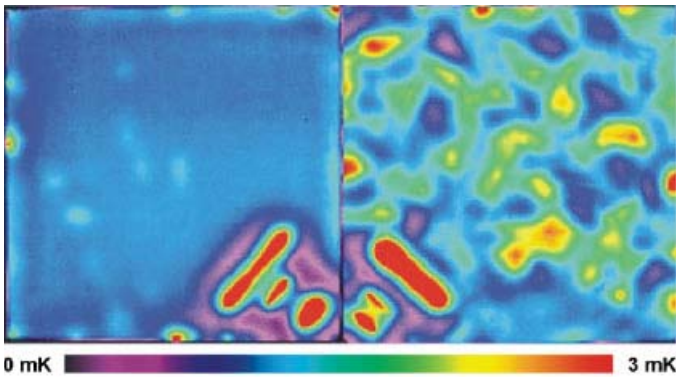

Figure 5. LimoLIT measurement after $POCl_3$ diffusion. Left: Cz-wafer, right: mc-wafer. The three line shaped shunts in the lower corners of both wafers are due to an intentionally scratched emitter after $POCl_3$ diffusion. The LimoLIT method allows a simultaneous measurement of both wafers as no contacting is needed (measurement time 14 h)

infrared LEDs (880 nm, Figure 5). The measurement was performed without additional constant bias light to achieve maximum signal-to-noise ratio. The signal shape was rectangular with a frequency of 15 Hz. Even in this early stage of processing the measurement reveals a lot of weak heat sources, mostly at the edges of the wafer, and in the case of the mc-wafer many heat sources are correlated to the grain structure.

The heat sources located in the lower corners are due to the artificial damage and are recognizable in the measurement of the finished solar cell as well (Figure 6). This proves that LimoLIT measurements can be used as a process-monitoring tool for single process steps. Doing so, even in the early stages of processing defects can be visualized and the wafer can be rejected, if necessary. As the measurement is contactless, there is no contamination due to the measurement itself.

The line-shaped structures close to the edges in Figure 6 are located at the joint between the rear Al contact and the remaining back-surface emitter. This emitter region was isolated by cutting off the edges and is therefore no more accessible by an *I–V* measurement, but it still collects carriers. Those carriers are drained by the direct connection to the base contact, reducing I_{sc} without affecting the shape of the *I–V* curve.

The *I–V* analysis of the solar cells shown in Figure 6 results in fill factors of 74% (Cz cell) and 75% (mc cell). Typical values for undamaged cells fabricated according to the process mentioned above are between 76–78%. As the damaged area is small compared with the entire cell area, the cell performance is only slightly affected.

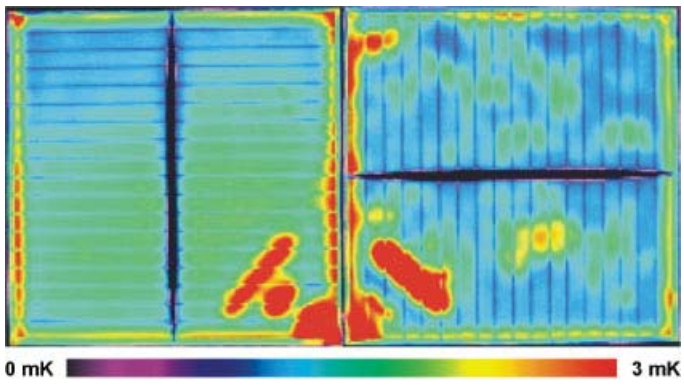

Figure 6. LimoLIT measurement (14 h) after processing the wafers shown in Figure 5 into solar cells. Left: Cz-wafer, right: mc-wafer. The modulation frequency is 15 Hz with a light intensity corresponding to a voltage of 575 mV (same light intensity and measurement time as used for the measurement shown in Figure 5). Especially for the mc-wafer many correlations between the signals in Figures 5 and 6 can be found as well as for the already mentioned damaged emitter for both cells

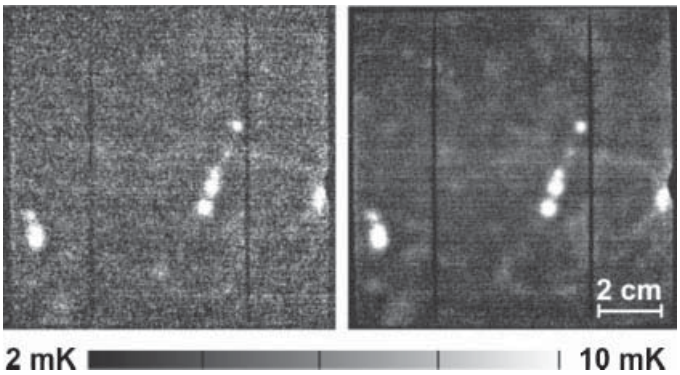

Figure 7. Comparison of a fast (2 s, left, $\sigma = 2{\cdot}2$ mK) and a high-quality (2 h, right, $\sigma = 0{\cdot}037$ mK) LimoLIT measurement of a $12{\cdot}5 \times 12{\cdot}5$ cm screen-printed industrial mc Si solar cell. Modulation frequency was 7·5 Hz. All major shunts are visible in the fast measurement

The spatially resolving LimoLIT method clearly identifies even small defect areas with high sensitivity. This, together with the possibility of measuring the wafer at any time after emitter formation, enables accurate damage location and tracking in industrial solar cell production.

RAPID SHUNT DETECTION

The typical lock-in behaviour according to Equation (4) gives a low-quality thermal image within a few seconds. Longer measurements differ in phase stability and background noise level, whereas large signal components remain nearly unchanged. To demonstrate this effect, Figure 7 shows a comparison of a high-quality (2 h) and a fast (2 s) measurement. Two seconds are enough to detect most of the shunts visible in the high quality image. The solar cell presented in Figure 7 exhibits a reduced fill factor (75% instead of the expected 77%), which can be attributed to shunts visualized within 2 s. High-speed and contactless measurement gives LimoLIT the potential for in-line process control.

CONCLUSION

The new LimoLIT technique is very well suited to localize heat dissipating defects in *pn*-structures. Based on conventional voltage-modulated lock-in thermography, one of the main advantages is the fact that no electrical contacts are needed, enabling a process monitoring sensitive to shunts even in the early stages of processing. The method is very sensitive and can reveal shunts well before they affect *I–V* characteristics significantly. An optional DC bias light provides realistic working conditions for the device. The lock-in technique is sufficiently fast and effective to detect stronger shunts in a few seconds, enabling in-line process control. The combination of an electric load together with a constant-bias light will simulate normal operation condition of solar cells even better.

Acknowledgements

Part of this work was funded by the EC in the RGSells project (ENK6-CT-2001-00574) and the German BMU in the frame of the ASiS project (0329846J). We wish to thank InfraTec for technical support and O. Breitenstein for fruitful and stimulating discussions.

REFERENCES

1. Rogalski A, Chrzanowski K. Infrared devices and techniques. *Opto-electronics Review* 2002; **10**(2): 111–136.
2. Dauner M, Bücher K. *Proceedings of the 26th IEEE PVSC*, Anaheim, 1997; 1137–1140.
3. Breitenstein O, Langenkamp M. *Lock-in Thermography, Basics and Use for Functional Diagnostics of Electronic Components.* Springer: Berlin, Heidelberg, New York, 2003.
4. Breitenstein O, Langenkamp M. *Proceedings of the 2nd WC PVSEC*, Vienna, 1998; 1382–1385.
5. Pernau T, Fath P, Bucher E. *Proceedings of the 29th IEEE PVSC*, New Orleans, 2002; 442–445.
6. Maldague XPV. *Theory and Practice of Infrared Technology for Nondestructive Testing*. Wiley: New York, 2001.
7. Stryi-Hipp G, Schoenecker A, Schitterer K, Bücher K, Heidler K. Precision spectral response and *I–V* characterisation of concentrator cells. *Proceedings of the 23rd IEEE PVSC*, Louisville, 1993; 303–308.
8. Schoenecker A, Zastrow A, Bücher K. Accurate spectral response measurement of non-linear high-efficiency solar cells, *Proceedings of the 12th EC PVSEC*, Amsterdam, 1994; 500–503.
9. Aberle AG, Schmidt J, Brendel R. On the data analysis of light-biased photoconductance decay measurements. *Journal of Applied Physics* 1996: **79**(3): 1491–1496.
10. Hahn G, Seren S, Sontag D, Gutjahr A, Laas L, Schönecker A. *Proceedings of the 3rd WC PVSEC*, Osaka, 2003; 1285–1288.